Special Collection

Catalytic Hydrogenation of Trivinyl Orthoacetate: Mechanisms Elucidated by Parahydrogen Induced Polarization

Andrey N. Pravdivtsev[+],*[a] Arne Brahms[+],[b] Stephan Kienitz,[b] Frank D. Sönnichsen,[b] Jan-Bernd Hövener[+],[a] and Rainer Herges[+]*[b]

Parahydrogen (pH_2) induced polarization (PHIP) is a unique method that is used in analytical chemistry to elucidate catalytic hydrogenation pathways and to increase the signal of small metabolites in MRI and NMR. PHIP is based on adding or exchanging at least one pH_2 molecule with a target molecule. Thus, the spin order available for hyperpolarization is often limited to that of one pH_2 molecule. To break this limit, we investigated the addition of multiple pH_2 molecules to one precursor. We studied the feasibility of the simultaneous hydrogenation of three arms of trivinyl orthoacetate (TVOA) intending to obtain hyperpolarized acetate. It was found that semihydrogenated TVOA underwent a fast decomposition accompanied by several minor reactions including an exchange of geminal methylene protons of a vinyl ester with pH_2. The study shows that multiple vinyl ester groups are not suitable for a fast and clean (without any side products) hydrogenation and hyperpolarization that is desired in biochemical applications.

1. Introduction

Magnetic resonance (MR) is a versatile physical effect that is widely used in science and clinical medicine. Its applications span from the analysis of a protein structure with a sub-Angstrom precision and microseconds time scale[1,2] to anatomical and physiological imaging.[3–6] Some applications, like measuring metabolites,[7] are severely hampered by the low sensitivity of the technique or a low signal-to-noise ratio (SNR). To address these shortcomings, the sensitivity of MR was increased steadily by hardware developments. About one order of magnitude in signal gain can be reached using cryoprobes[8,9] or cryomagnets with higher magnetic fields.[10,11]

Nuclear spin hyperpolarization is a family of methods that brings a 10 to 10^5 fold signal gain using physical or chemical effects.[12–15] Instead of improving the detection electronics[16,17] or increasing the magnetic field, these methods use special techniques to increase the polarization of the spins directly.[18–20]

Parahydrogen based methods employ the highly ordered spin state of parahydrogen (pH_2) to achieve net polarization of a target molecule. To do so, a pH_2 molecule is either added to a target molecule by a catalytic hydrogenation reaction (Figure 1),[20] or exchanged[37].

Parahydrogen and synthesis allow dramatically enhanced nuclear alignment (PASADENA) is an experiment that exploits pH_2 hydrogenation at high magnetic fields.[21] The unique property of PASADENA is its *anti-phase* shape of spectral lines in the basic excitation and acquisition NMR experiment, while normal or thermal MR resonances are always *in-phase*. This feature is used to study hydrogenation routes and also reveals a fraction of pairwise hydrogenation.[22] The advantage of PHIP as a hyperpolarization method is its cost-efficiency: with only little investment,[23–25] highly polarized samples can be produced in a batch process[26,27] or continuously.[28]

Although PHIP has many powerful features, its scope was restricted until recently to a few organic molecules with few biochemical applications.[29] The utilization of functionalized vinyl or propargyl groups, so-called PHIP side arm hydrogenation (PHIP-SAH) enabled new applications. Here, a side arm is hydrogenated and then polarization is transferred to the target site of the polarized molecule, which often is the ^{13}C nucleus of a carboxyl group. PHIP-SAH has enabled hyperpolarization of a larger number of endogenous molecules including acetate (Figure 1a), pyruvate,[30] amino acids[31] and peptides.[32]

Recently, metabolites hyperpolarized with PHIP-SAH were tested in cell-cultures[33] and in vivo.[34] PHIP-SAH at high magnetic fields demonstrated more than 50% ^{13}C polarization of ethyl acetate-d_6 and 19% of acetate-d_3 within seconds.[35]

[a] Dr. A. N. Pravdivtsev,[+] Prof. Dr. J.-B. Hövener[+]
Section Biomedical Imaging
Molecular Imaging North Competence Center (MOIN CC)
Department of Radiology and Neuroradiology
University Medical Center Kiel, Kiel University
Am Botanischen Garten 14, 24114, Kiel, Germany
E-mail: andrey.pravdivtsev@rad.uni-kiel.de
[b] A. Brahms,[+] S. Kienitz, Prof. Dr. F. D. Sönnichsen, Prof. Dr. R. Herges[+]
Otto Diels Institute for Organic Chemistry, Kiel University
Otto Hahn Platz 5, 24098, Kiel, Germany
E-mail: rherges@oc.uni-kiel.de
[+] These authors contributed equally to this work

Supporting information for this article is available on the WWW under https://doi.org/10.1002/cphc.202000957

Special Collection An invited contribution to a Special Collection on Parahydrogen Enhanced Resonance

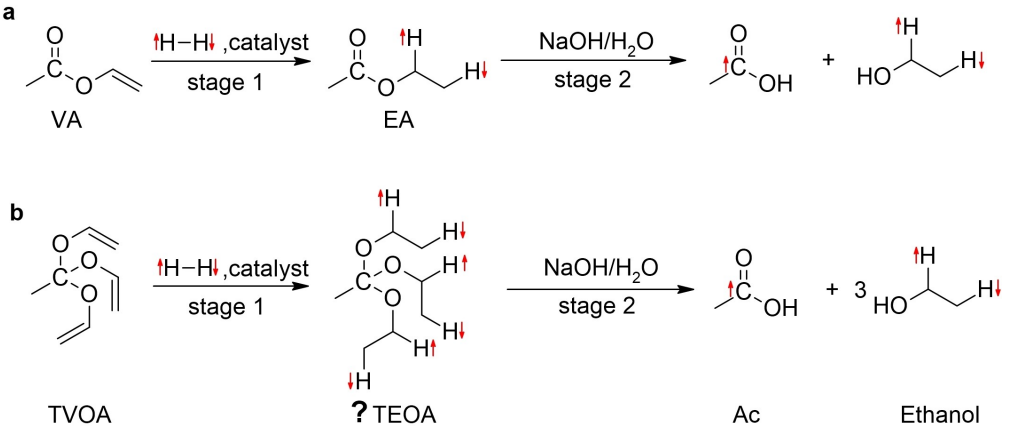

Figure 1. Reaction schemes of hydrogenation and side-arm cleavages confirmed for PHIP-SAH (a) and expected (marked with "?") for PHIP-HOT (b). (a) Hydrogenation of vinyl acetate (VA) results in the production of ethyl acetate (EA). The cleavage of the ester in the presence of a base and water leads to acetate (Ac) and ethanol. (b) Hydrogenation of trivinyl orthoacetate (TVOA) with three pH_2 molecules is expected to lead to triethyl orthoacetate (TEOA). The cleavage of ethyl groups in the presence of NaOH and water was expected to result in acetate (Ac) and three molecules of ethanol. In both cases, only acetate and ethanol would be the products. Note that full hydrogenation of TVOA was assumed. Red arrows indicate expected hyperpolarized spins: ethanol is polarized because of the chemical reaction of the vinyl group with pH_2. Optionally, polarization may be transferred from ethyl to ^{13}C after hydrogenation that is indicated by the arrow next to C of acetate.[34,35] It has been shown experimentally that rapid TEOA dissociation occurs during stage 1, i.e. without adding NaOH. TVOA hydrogenation with $[Rh(dppb)(COD)]BF_4$ catalyst was studied here in details.

Still, there is much room to improve the polarization level of PHIP. While exchange based methods[36,37] allow continuous re-hyperpolarization of the target molecule,[38] the spin order available to hydrogenation-based methods to polarize the target is limited to a single pH_2 molecule.

Thus, we investigated the question, whether multiple pH_2 molecules can be added to a target molecule and used for its hyperpolarization. We pursued the hypothesis that multiple hydrogenations of the same molecule with pH_2 will lead to a higher level of polarization of the target fragment.

Towards this goal, we introduce a new experiment: PHIP by hydrogenation of three sidearms (PHIP-HOT, Figure 1b). Here, the target fragment (acetate) is functionalized with three equivalent vinyl groups, resulting in trivinyl orthoacetate (TVOA).

Employing a reaction similar to PHIP-SAH, we aimed at hyperpolarizing the same molecule, acetate. Contrary to our expectations, however, an entirely different reaction took place. These findings are reported in this paper.

2. Results

PASADENA experiments (Figure 1b, stage 1) were conducted with TVOA and catalyst $[Rh(dppb)(COD)]BF_4$ = **[1]** (CAS: 79255-71-3) at 25 °C and ambient pressure with 0.2 bar pH_2 over-pressure in acetone-d_6. Enhanced, PASADENA-type anti-phase signals were observed for the following molecules (Figures 2 and 3): ethyl acetate (EA), ethanol, acetaldehyde, vinyl acetate (VA), H_2 and other unassigned products. After 5 minutes of constant H_2 bubbling, high-resolution NMR spectra were acquired. A ratio of [EA]:[acetaldehyde]:[ethanol] = 1:1.95:0.2 was found. 2-Chloroethanol and cyclooctene were also found. 2-Chloroethanol was used in the synthesis of TVOA (see Experimental Section) and traces thereof were found in the pre-hydrogenation sample. Cyclooctene is the side product of the catalyst **[1]** activation. It is formed by hydrogenation of the 1,5-cyclooctadiene ligand of the Rh-catalyst. Note that triethyl orthoacetate or any semi-hydrogenated TVOA, i.e. divinyl ethyl orthoacetate, were not found.

The experiment was repeated in chloroform-d. EA was found to be polarized to a much higher level, while ethanol was polarized to a lesser extend. The concentration ratio of the products of the TVOA hydrogenation and decomposition was determined by NMR after 20 minutes of H_2 bubbling [EA]:[acetaldehyde]:[VA]:[ethanol] = 1:2.15:0.42:0.04. Strongly polarized resonances of VA appeared; all these resonances exhibited the PASADENA-type spectrum.

Rapid decomposition of the substrate after hydrogenation may occur due to residual water and acids; possible decomposition paths are discussed later (Figure 4). To reduce this effect, we additionally purified the solvents by pouring acetone-d_6 through a dry magnesium sulfate powder and chloroform-d through a dry basic aluminium oxide powder column, directly before sample preparation. This filtration did not change our observations.

3. Discussion

3.1. Polarization of Ethyl Acetate and Ethanol

A molecule with three unsaturated side arms TVOA was successfully synthesized and subjected to a PASADENA experiment. Experimentally, TVOA was found to be stable in the presence of **[1]** and dissociation started only after the addition of H_2.

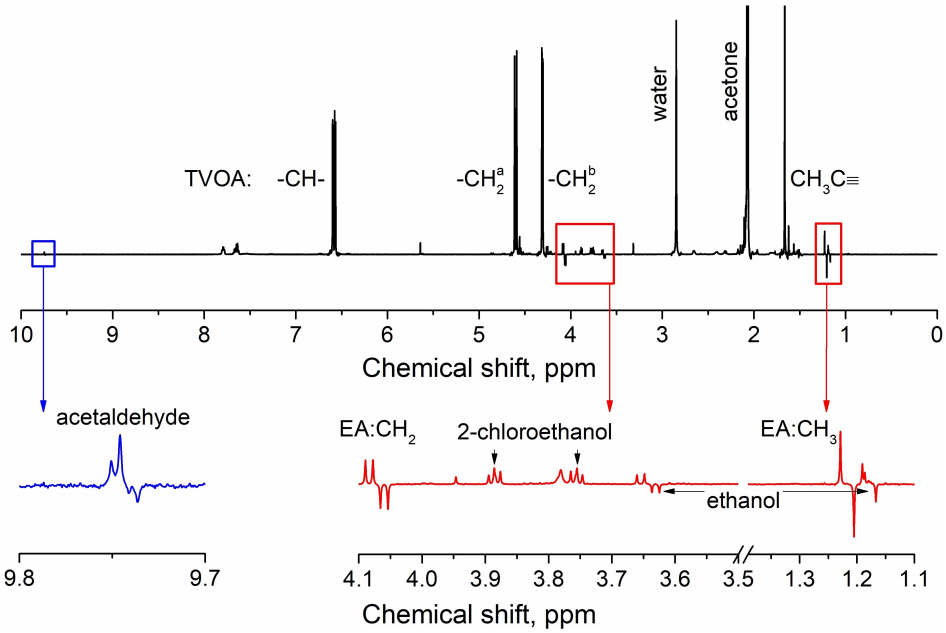

Figure 2. ^{1}H NMR spectrum of TVOA hydrogenated with pH_2 and [**1**] in acetone-d_6 at 14.1 T. The main polarized product identified was ethyl acetate (EA). Ethanol and acetaldehyde showed much less polarization. Other side products were 2-chloroethanol, cyclooctene and various unassigned alkanes. Note that cyclooctene is the side product of the catalyst activation and subsequent hydrogenation of 1,5-cyclooctadiene. Relevant sections of the spectrum with hyperpolarized signals are magnified.

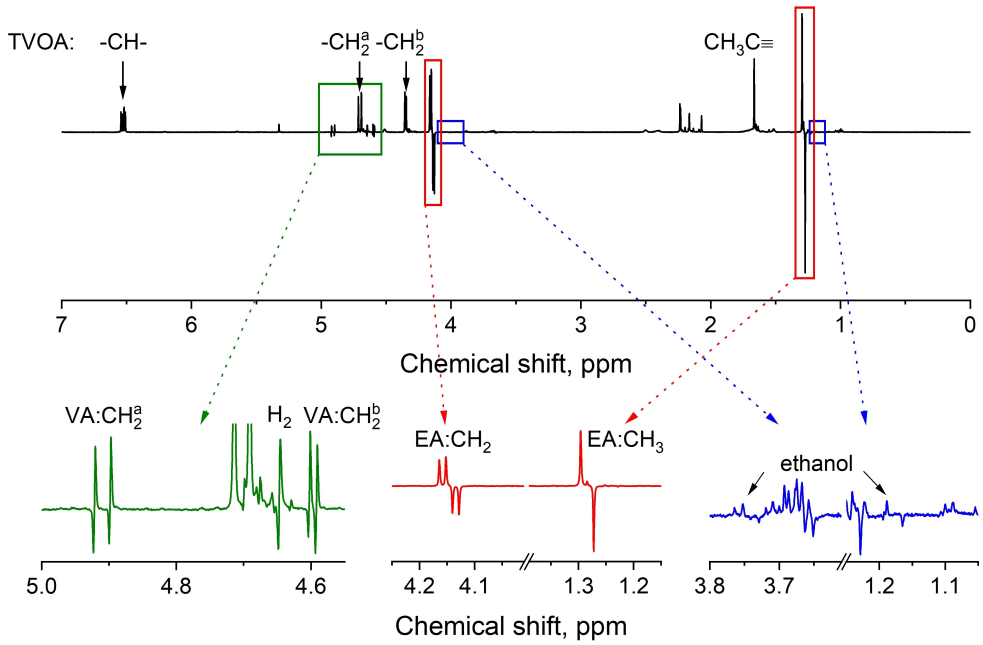

Figure 3. ^{1}H NMR spectrum of TVOA hydrogenated with pH_2 and [**1**] in chloroform-d at 14.1 T. Relevant sections of the spectrum with hyperpolarized signals are magnified. The main polarized product identified was ethyl acetate (EA). Ethanol, acetaldehyde, vinyl acetate (VA) and H_2 showed much less polarization than EA. Note the partially negative line of H_2 and polarized antiphase lines of CH_2 protons of VA. Other side products were 2-chloroethanol, cyclooctene and various unassigned alkanes. Note that cyclooctene is the side product of the catalyst activation and subsequent hydrogenation of 1,5-cyclooctadiene.

NMR showed multiple PASADENA signals but no signals from semi or fully hydrogenated TVOA (Figure 1–3). Because no hyperpolarized orthoacetate signals were observed, we assume that after the first hydrogenation the product immediately dissociated.

Divinyl ethyl orthoacetate (DVEOA) should be the first product of TVOA hydrogenation and we suggest three main pathways how it can dissociate in the presence of water (Figure 4). First, a proton will activate one of the three ether side arms of DVEOA. If the hydrogenated sidearm (ethyl) is

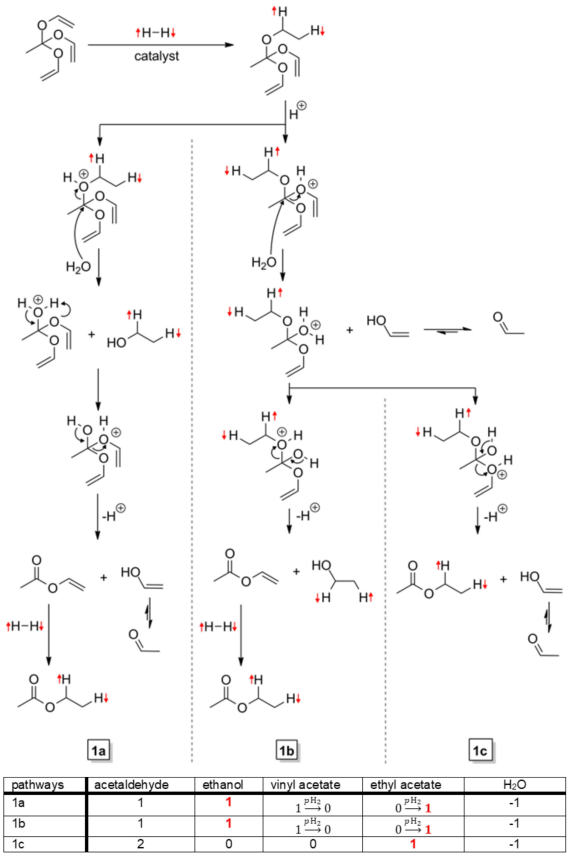

pathways	acetaldehyde	ethanol	vinyl acetate	ethyl acetate	H_2O
1a	1	1	$1 \xrightarrow{pH_2} 0$	$0 \xrightarrow{pH_2} 1$	-1
1b	1	1	$1 \xrightarrow{pH_2} 0$	$0 \xrightarrow{pH_2} 1$	-1
1c	2	0	0	1	-1

Figure 4. Potential reactions of TVOA disintegration in presence of water after hydrogenation with pH_2 and [**1**], and corresponding table of products. We assume that hydrogenation of TVOA results in divinyl ethyl ortho acetate (DVEOA) with a polarized ethyl group. Three cleavage pathways are considered here. If the hyperpolarized ethyl ether sidearm is cleaved first, this will lead to vinyl acetate, acetaldehyde and hyperpolarized ethanol (**1 a**). If the vinyl ether is cleaved first, then either the products will be the same (**1 b**) or two molecules of acetaldehyde and hyperpolarized ethyl acetate will be produced (**1 c**). Red arrows in the scheme and numbers in the table indicate hyperpolarized protons and molecules by hydrogenation with pH_2. This cleavage scheme explains only polarization of ethyl acetate and ethanol.

activated the dissociation will lead to hyperpolarized ethanol (Figure 4, **1 a**).

The other possibility is that one of the unsaturated sidearms (vinyl) of DVEOA is activated (Figure 4, **1 b** and **1 c**). In this case, the dissociation could lead to hyperpolarized ethanol (**1 b**) or hyperpolarized ethyl acetate (EA, **1 c**). Note that emerging VA in **1 a** and **1 b** could also be hydrogenated and hence polarized EA will be produced. All products of TVOA hydrogenation and consequent dissociation pathways are summarized in the table (Figure 4).

These possible pathways allow only EA or ethanol to be polarized. Experimentally, fractions of EA and ethanol were changing with the duration of bubbling; therefore, we could not unequivocally determine a major pathway. However, it appears that EA experiences a stronger polarization than ethanol (i) and the obtained concentration ratio [acetaldehyde]:[ethyl acetate] is close to 2:1 (ii). Both facts indicate that the reaction path **1 c** is preferred (Figures 2 and 3), despite the signal ratios being different in two solvents. The consumption of the H_2O residues is one possible reason for the product distribution varying with time.

3.2. Polarization of Vinyl Acetate

The PASADENA type polarization of CH_2-protons of vinyl acetate (VA, Figure 3) is a rather uncommon effect. It can be explained by the pairwise exchange of CH_2-protons with pH_2 on the transient complex, which consists of [**1**], TVOA and pH_2 (Figure 5). The result of this hydrogen exchange is a TVOA with a terminal hyperpolarized sidearm. If this TVOA undergoes normal hydrogenation and dissociation on the pathways **1 a** or **1 b** (Figure 4), a terminal hyperpolarized VA is obtained. The minor level of polarization (Figure 3) indicates that it is not the major polarization mechanism.

It should be noted that only the unique signal enhancement caused by pH_2 addition allowed us to find this exchange of H_2 on geminal protons of TVOA. It would have been impossible with the normal H_2. A similar effect was observed also by Bargon et al.[39,40] when using rhodium and palladium catalysts to hydrogenate styrene. In both cases, the structure of the substrate results in the formation of a relatively long-lived intermediate. This is due to the coordination of the benzene

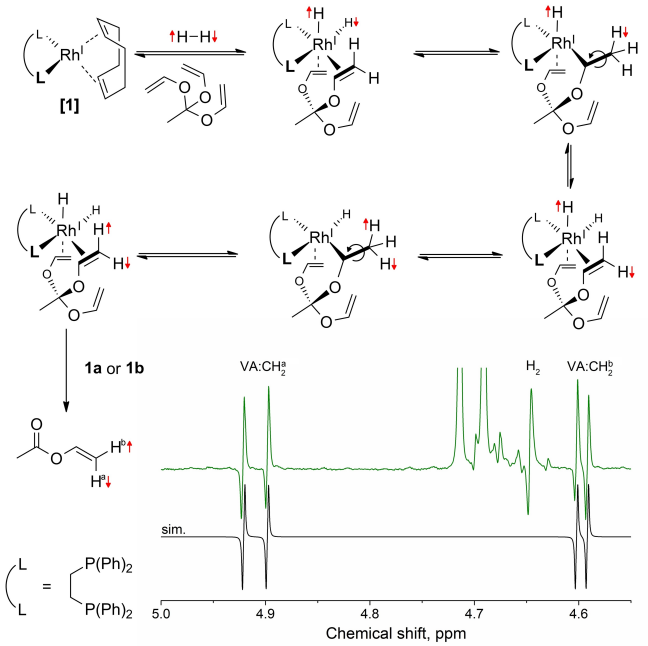

Figure 5. Trivinyl orthoacetate – H_2 exchange with experimental and simulated (sim.) PASADENA spectra. TVOA exchanges its methylene protons with pH_2 when both (hydrogen and TVOA) are coordinating to [**1**]. After dissociation according to pathway 1a or 1b, vinyl acetate (VA) with polarized CH_2-protons is produced. The following NMR parameters were used for simulations of polarized VA (sim.): chemical shifts: $\delta_{CH} = 7.267$ ppm, $\delta_{CH_2^a} = 4.85$ ppm, $\delta_{CH_2^b} = 4.59$ ppm and J-coupling constants: $^3J_{CH-CH_2^a} = 13.9$ Hz, $^3J_{CH-CH_2^b} = 6.34$ Hz, $^2J_{CH_2} = -1.4$ Hz. It was assumed that the CH_2 protons are produced by pH_2 (PASADENA effect, sim.). In the experiment and simulations nonselective 45° excitation RF-pulses were used.

ring of styrene[39,40] or due to the coordination of a second vinyl group of TVOA to the metal ion, which leads to hyperpolarization of the geminal protons.

3.3. Polarization of Acetaldehyde

The PASADENA type polarization of the CH-proton of acetaldehyde (AD) is another unexpected hyperpolarized signal (Figure 2). Although it is a saturated aldehyde, its origin is unsaturated vinyl alcohol, which was not hydrogenated by pH_2. The tentative pathway that leads to the polarization of AD is a pairwise exchange of CH and one CH_2 proton of the vinyl group of TVOA with pH_2 on **[1]** (Figure 6). This unconventionally polarized TVOA would lead to the observed polarized acetaldehyde after the dissociation pathways **1a**, **1b** or **1c** (Figure 4). This vicinal pairwise hydrogen exchange is an H_2 exchange mechanism occurring in addition to the previously discussed exchange of geminal protons with pH_2 (Figure 5). Similar vicinal pH_2 exchange was observed by Skovpin et al.[41] in the hydrogenation reaction of propylene with a silica-immobilized Rh catalyst.

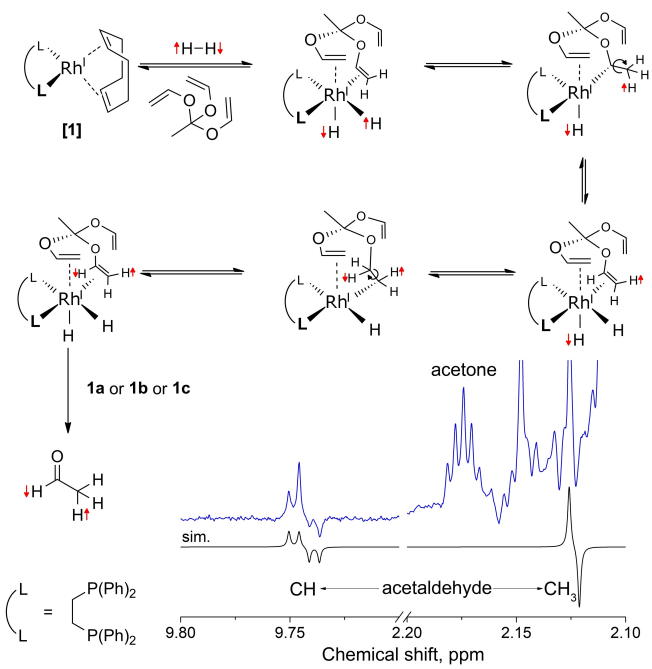

Figure 6. Acetaldehyde exchange reaction pathway with experimental and simulated (sim.) PASADENA spectra. TVOA exchanges one of its CH_2-protons and its CH-proton with pH_2 when both (hydrogen and TVOA) are coordinating to **[1]**. The hydrogenation and dissociation of this hyperpolarized TVOA would lead to the observed polarized acetaldehyde. The following NMR parameters were used for simulations of polarized acetaldehyde: chemical shifts: $\delta_{CH} = 9.7435$ ppm, $\delta_{CH_3} = 2.123$ ppm and J-coupling constants: $^3J_{CH-CH_3} = 2.85$ Hz. It was assumed that the CH and one of CH_3 protons are resulting from pH_2 (PASADENA effect, sim.). In the experiment and simulations nonselective 45° excitation RF-pulses were used.

3.4. Polarization of H_2

A partial negative line (PNL)[42,43] was observed on H_2 in chloroform after hydrogenation of TVOA with **[1]** (Figure 3). This is a good indicator of a slow catalytic hydrogenation when pH_2 is not completely consumed by the catalyst but rather exchanges: $[M] + H_2 \leftrightarrow [M] - H_2$. Here $[M]$ stands for a metal complex or catalyst. When pH_2 associates with $[M]$, its spin order starts evolving in a so-called singlet-triplet conversion. If this hydride dissociates instead of hydrogenating a substrate, it manifests itself as H_2 with a PNL. One of the possible steps, where this can happen, is the $pH_2 \leftrightarrow H_2$ exchange, when vinyl acetate or acetaldehyde are polarized (Figures 5 and 6) where [M] stands for [TVOA-**[1]**] complex.

4. Conclusions

The attempt to hydrogenate all three double C=C bonds of TVOA was not successful. Ethyl acetate was the main product of hydrogenation and not the expected products divinyl ethyl orthoacetate or other orthoacetate derivatives. TVOA was cleaved immediately in the presence of H_2 and **[1]**. Even the removal of acid traces in the solvents by filtration over a basic Al_2O_3 column did not stop the instant decomposition of DVEOA. Decomposition of DVEOA leads to the production of polarized ethyl acetate, vinyl acetate, acetaldehyde, ethanol and H_2.

Hence, the studies show that TVOA is not well suited for the hydrogenation of "many side-arms". We assume that a similar approach will be also not successful for hyperpolarization of pyruvate, because three (or two) vinyl groups will coordinate to the metal complex (catalyst), which will slow down the hydrogenation reaction; possibly side-reactions and products will be observed similar to those that have been identified in this study.

PASADENA proved to be key to elucidate the underlying reaction mechanism. Without the unique line shape, the pairwise H_2 exchange of the geminal protons of vinyl acetate and the vicinal protons of acetaldehyde would have remained unrecognized.

This is yet another proof that labelling with pH_2 is a unique tool to distinguish the pathways in hydrogenation reactions; – PHIP provides a sophisticated analytical tool for the elucidation of hydrogenation mechanisms, catalysis and other elementary chemical reactions.

Experimental Section

Sample Preparation

Samples for PHIP–SAH and –HOT: 10 µl of TVOA (synthesized according to a protocol described below) or vinyl acetate (CAS 108-05-4, Merck) was dissolved in 600 µL of acetone-d_6 or chloroform-d (Deutero GmbH) yielding a 100 mmol/L concentration. For PHIP experiments the catalyst [1,4-Bis(diphenylphosphino)butane(1,5-cyclooctadiene)rhodium(I) tetrafluoroborate] **[1]** (CAS: 79255-71-3, Strem Chemicals) was added to reach a concentration of 5 mmol/L.

Chloroform-d and acetone-d_6 were dried by pouring it through a 3 cm column (ID = 5 mm) of basic aluminium oxide powder and magnesium sulfate respectively directly before preparation of the samples. Both powders were dried overnight at 120°. Note, that even after drying, the residual HDO concentration was determined to approx. 1 mM. These samples were flushed by pH_2 to produce hyperpolarization in the following stage.

Samples for reference NMR spectra: NMR spectra of the following compounds dissolved in chloroform-d or acetone-d_6 were measured at concentrations of 10–100 mM: vinyl acetate (CAS: 108-05-4), ethyl-acetate (CAS: 141-78-6), triethyl orthoacetate (CAS: 78-39-7), acetaldehyde (CAS: 75-07-0), 2-chloroethanol (CAS: 107-07-3), ethyl alcohol (CAS: 64-17-5). All compounds were purchased from Merck. These samples and the corresponding spectra were used to assign the products of the TVOA hydrogenation.

Synthesis

TVOA was synthesized according to the protocol in Ref. [44] with some modifications. The implemented protocol consisted of 2 steps (Figure 7).

Synthesis of tris(chloroethyl)orthoacetate: Trichloroacetic acid (500 mg, 3.06 mmol, CAS: 76-03-9, Merck) was placed in a 2-necked flask with a rubber septum on a short way distillation apparatus. The trichloroacetic acid was dried under reduced pressure (7 mbar) for 3 h. Then the flask was flushed with nitrogen and 10 mL of trimethyl orthoacetate (8.56 g, 71.3 mmol, CAS: 78-39-7, TCI GmbH) was added. The reaction mixture was heated to 90 °C and 3 mL of 2-chloroethanol (CAS: 107-07-3, Merck) was added to the flask. The pressure was carefully reduced to 500 mbar and further 2-chloroethanol (3 ml) was added every 0.5 h for 2.5 h until a total of 15 ml was reached (17.0 g, 220 mmol). The reaction mixture was heated to 90 °C for 3 h. During this time 7.12 g of methanol was distilled from the reaction mixture. The heating bath was then removed and replaced with an ice bath. 400 mg of potassium *tert*-butoxide (CAS: 865-47-4, TCI GmbH) dissolved in 5 ml dry methanol (CAS: 67-56-1, Merck) was added to quench the reaction. The product was obtained by distillation from the reaction mixture as a colorless oil (6.84 g, 43.80 mmol, bp. 155 °C at 7 mbar). This corresponds to a yield of 62% relative to the trimethyl orthoacetate deployed.

Synthesis of trivinyl orthoacetate (TVOA): Sodium hydride (60% suspension in mineral oil) (2.20 g, 54.32 mmol, CAS: 7646-69-7, Acros) was mixed with 5 mL 1,2-dimethoxyethane (CAS: 110-71-4, ABCR) under a nitrogen atmosphere in a 3-neck flask with a rubber septum. Then *tert*-butanol (234 mg, 3.16 mmol, CAS: 75-65-0, Grüssing) was added at room temperature and the suspension was stirred for 5 min. Tris(chloroethyl)orthoacetate (4.41 g, 15.09 mmol) was carefully added to the solution, which was heated under reflux for 5 h. The solvent was removed under reduced pressure (50 mbar, 40 °C). The residue was treated with 30 mL of diethyl ether (CAS: 60-29-7, Walter-CMP) and 20 mL of distilled water. The phases were separated and the organic phase was washed three times with 20 ml of water and dried over magnesium sulfate (CAS: 7487-88-9, Grüssing). The solvent was removed under reduced pressure and the remaining liquid was distilled two times at reduced pressure yielding TVOA (358 mg, 2.28 mmol, 80 °C at 30 mbar) with a purity of 90%. This corresponds to a yield of 15% based on tris(chloroethyl) orthoacetate. Possible impurities and side products are bisvinyl (chloroethyl)orthoacetate, 2-chloroethanol (Figure 8).

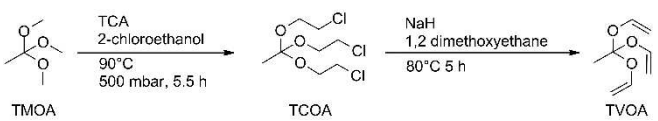

Figure 7. Trivinyl orthoacetate (TVOA) synthesis. Step 1: the methyl ethers of trimethyl orthoacetate (TMOA) are replaced by chloroethyl under acidic conditions to give the tris(chloroethyl)orthoacetate (TCOA). Step 2: sodium hydride is used as a base in an elimination reaction to obtain TVOA.

Experimental Routines

PASADENA experiments: pH_2 was prepared using a liquid nitrogen setup that provides the pH_2 fraction of 50%.[45] All experiments were carried out on a 600 MHz NMR spectrometer (Bruker Avance II) with a cryogenically cooled probe (TCI) and 5 mm screw-cap NMR tubes (Wilmad). The gas was delivered into the spectrometer by a 1/16" polytetrafluoroethylene (PTFE) capillary (0.023" internal diameter). A hollow optical fiber (Molex, part. num. 106815-0026, 250 μm internal diameter, 360 μm outer diameter) was glued with instant 2-component adhesive (Loctite 3090, Henkel) to the end of the capillary and inserted into the NMR tube and solution. The used hollow fiber is resistant to aggressive media and does not cause magnetic field distortion: the increase of FWHM after field shimming is below 1 Hz. The pressure was set to about 1.2 bar (0.2 bar overpressure to atmospheric pressure) and adjusted to achieve a steady bubbling. For the experiments, pH_2 was supplied (bubbled) to the sample solution for 10–30 s to generate PASADENA. Next, the bubbling was stopped and the system was allowed to settle down for another 2 s. After that, a PASADENA spectrum was recorded after 45° excitation. All NMR experiments were carried out at 25 °C and ambient pressure.

Mass spectrometric analysis. Using the same H_2 bubbling setup, the PHIP samples were flushed with pH_2 at room temperature for 5–10 minutes in 5 ml amber glass vials. Using a Jeol AccuTOF GCv 4G spectrometer with electron ionisation (EI), mass spectra of the blank samples (before hydrogenation) and corresponding samples after hydrogenation were acquired (cf. SI). No stable products of direct TVOA hydrogenation, namely DVEOA or TEOA were found.

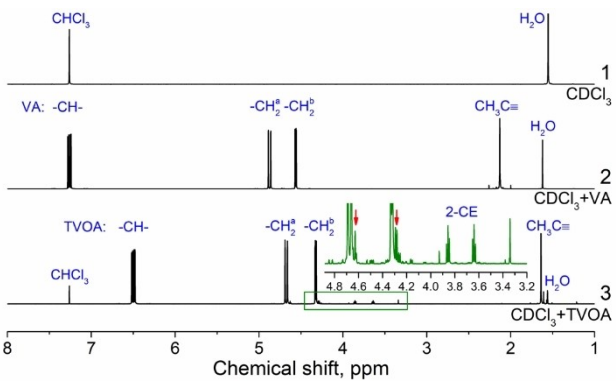

Figure 8. High-resolution ^{1}H NMR spectra of chloroform-d (1), vinyl acetate (VA, 2) and trivinyl orthoacetate (TVOA, 3) in chloroform-d. Red arrows indicate side products of synthesis (presumably it is bisvinyl (chloroethyl)orthoacetate). 2-Chloroethanol (2-CE) and some other residues from the synthesis are also present. The estimated purity of TVOA is about 90%.

Supporting Material

TOCSY and mass-spectra of the analyzed system (PDF). the Matlab simulation source code and raw NMR spectra (TopSpin files, .zip) are available as supplementary.

Abbreviations

TVOA	trivinyl orthoacetate
DVEOA	divinyl ethyl orthoacetate
TEOA	triethyl orthoacetate
TCA	trichloro acetic acid
TMOA	trimethyl orthoacetate
TCOA	tri(chloroethyl) orthoacetate
VA	vinyl acetate
EA	ethyl acetate
AD	acetaldehyde
CE	chloroethanol
PHIP	parahydrogen induced polarization
PHIP-SAH	PHIP-side arm hydrogenation
PHIP-HOT	PHIP by hydrogenation of three side arms

Acknowledgements

We acknowledge support by the Emmy Noether Program "metabolic and molecular MR" (HO 4604/2-2), the research training group "materials for brain" (GRK 2154/1-2019), DFG – RFBR grant (HO 4604/3-1, N° 19-53-12013), the German Federal Ministry of Education and Research (BMBF) within the framework of the e:Med research and funding concept (01ZX1915 C), cluster of Excellence "precision medicine in inflammation" (PMI 1267). Kiel University and the Medical Faculty are acknowledged for supporting the Molecular Imaging North Competence Center (MOIN CC) as a core facility for imaging in vivo. MOIN CC was founded by a grant from the European Regional Development Fund (ERDF) and the Zukunftsprogramm Wirtschaft of Schleswig-Holstein (Project no. 122-09-053). Open access funding enabled and organized by Projekt DEAL.

Conflict of Interest

The authors declare no conflict of interest.

Keywords: geminal hydrogenation · homogeneous catalysis · hyperpolarization · parahydrogen · sidearm hydrogenation

[1] M. Sattler, J. Schleucher, C. Griesinger, *Prog. Nucl. Magn. Reson. Spectrosc.* **1999**, *34*, 93–158.
[2] O. F. Lange, N.-A. Lakomek, C. Farès, G. F. Schröder, K. F. A. Walter, S. Becker, J. Meiler, H. Grubmüller, C. Griesinger, B. L. de Groot, *Science* **2008**, *320*, 1471–1475.
[3] A. Haase, J. Frahm, D. Matthaei, W. Hänicke, K.-D. Merboldt, *J. Magn. Reson.* **1986**, *213*, 533–541.
[4] G. H. Glover, *Neurosurg. Clin. N. Am.* **2011**, *22*, 133–139.
[5] B. Witulla, N. Goerig, F. Putz, B. Frey, T. Engelhorn, A. Dörfler, M. Uder, R. Fietkau, C. Bert, F. B. Laun, *PLoS One* **2020**, *15*, e0227146.
[6] T. Gerhalter, L. V. Gast, B. Marty, M. Uder, P. G. Carlier, A. M. Nagel, *NMR Biomed.* **2020**, *33*, e4279.
[7] V. Xu, H. Chan, A. P. Lin, N. Sailasuta, S. Valencerina, T. Tran, J.-B. Hövener, B. D. Ross, *Semin. Neurol.* **2008**, *28*, 407–422.
[8] M. Sack, F. Wetterling, A. Sartorius, G. Ende, W. Weber-Fahr, *NMR Biomed.* **2014**, *27*, 709–715.
[9] T. Niendorf, A. Pohlmann, H. M. Reimann, H. Waiczies, E. Peper, T. Huelnhagen, E. Seeliger, A. Schreiber, R. Kettritz, K. Strobel, M.-C. Ku, S. Waiczies, *Front. Pharmacol.* **2015**, *6*, DOI 10.3389/fphar.2015.00255.
[10] J. J. Suttie, L. DelaBarre, A. Pitcher, P. F. van de Moortele, S. Dass, C. J. Snyder, J. M. Francis, G. J. Metzger, P. Weale, K. Ugurbil, S. Neubauer, M. Robson, T. Vaughan, *NMR Biomed.* **2012**, *25*, 27–34.
[11] L. V. Gast, S. Völker, M. Utzschneider, P. Linz, T. Wilferth, M. Müller, C. Kopp, B. Hensel, M. Uder, A. M. Nagel, *Magn. Reson. Med.* **n.d.**, *n/a*, DOI 10.1002/mrm.28428.
[12] J. H. Ardenkjær-Larsen, B. Fridlund, A. Gram, G. Hansson, L. Hansson, M. H. Lerche, R. Servin, M. Thaning, K. Golman, *PNAS* **2003**, *100*, 10158–10163.
[13] J.-B. Hövener, A. N. Pravdivtsev, B. Kidd, C. R. Bowers, S. Glöggler, K. V. Kovtunov, M. Plaumann, R. Katz-Brull, K. Buckenmaier, A. Jerschow, F. Reineri, T. Theis, R. V. Shchepin, S. Wagner, P. Bhattacharya, N. M. Zacharias, E. Y. Chekmenev, *Angew. Chem. Int. Ed.* **2018**, *57*, 11140–11162; *Angew. Chem.* **2018**, *130*, 11310–11333.
[14] R. Kaptein, *Chem. Phys. Lett.* **1968**, *2*, 261–267.
[15] I. Schwartz, J. Scheuer, B. Tratzmiller, S. Müller, Q. Chen, I. Dhand, Z.-Y. Wang, C. Müller, B. Naydenov, F. Jelezko, M. B. Plenio, *Sci. Adv.* **2018**, *4*, eaat8978.
[16] U. Ludwig, A.-K. Eisenbeiss, C. Scheifele, K. Nelson, M. Bock, J. Hennig, D. von Elverfeldt, O. Herdt, T. Flügge, J.-B. Hövener, *Sci. Rep.* **2016**, *6*, 23301.
[17] V. V. Zhivonitko, V.-V. Telkki, J. Leppäniemi, G. Scotti, S. Franssila, I. V. Koptyug, *Lab Chip* **2013**, *13*, 1554–1561.
[18] G. Norquay, G. J. Collier, M. Rao, N. J. Stewart, J. M. Wild, *Phys. Rev. Lett.* **2018**, *121*, 153201.
[19] J. H. Ardenkjær-Larsen, S. Bowen, J. R. Petersen, O. Rybalko, M. S. Vinding, M. Ullisch, N. C. Nielsen, *Magn. Reson. Med.* **2019**, *81*, 2184–2194.
[20] K. V. Kovtunov, E. Pokochueva, O. Salnikov, S. Cousin, D. Kurzbach, B. Vuichoud, S. Jannin, E. Chekmenev, B. Goodson, D. Barskiy, I. Koptyug, *Chem. Asian J.* **2018**, *13*, 1857–1871.
[21] C. R. Bowers, D. P. Weitekamp, *J. Am. Chem. Soc.* **1987**, *109*, 5541–5542.
[22] K. V. Kovtunov, D. Burueva, L. Kovtunova, V. Bukhtiyarov, I. Koptyug, *Chem. Eur. J.* **2019**, *25*, 1420–1431.
[23] A. Gamliel, H. Allouche-Arnon, R. Nalbandian, C. M. Barzilay, J. M. Gomori, R. Katz-Brull, *Appl. Magn. Reson.* **2010**, *39*, 329–345.
[24] J.-B. Hövener, S. Bär, J. Leupold, K. Jenne, D. Leibfritz, J. Hennig, S. B. Duckett, D. von Elverfeldt, *NMR Biomed.* **2013**, *26*, 124–131.
[25] K. Jeong, S. Min, H. Chae, S. K. Namgoong, *Magn. Reson. Chem.* **2018**, *56*, 1089–1093.
[26] R. V. Shchepin, A. M. Coffey, K. W. Waddell, E. Y. Chekmenev, *J. Am. Chem. Soc.* **2012**, *134*, 3957–3960.
[27] S. Berner, A. B. Schmidt, M. Zimmermann, A. N. Pravdivtsev, S. Glöggler, J. Hennig, D. von Elverfeldt, J.-B. Hövener, *ChemistryOpen* **2019**, *8*, 728–736.
[28] A. N. Pravdivtsev, F. D. Sönnichsen, J.-B. Hövener, *ChemPhysChem* **2020**, *21*, 667–672.
[29] S. Bär, T. Lange, D. Leibfritz, J. Hennig, D. von Elverfeldt, J.-B. Hövener, *J. Magn. Reson.* **2012**, *225*, 25–35.
[30] F. Reineri, T. Boi, S. Aime, *Nat. Commun.* **2015**, *6*, ncomms6858.
[31] L. Kaltschnee, A. P. Jagtap, J. McCormick, S. Wagner, L.-S. Bouchard, M. Utz, C. Griesinger, S. Glöggler, *Chem. Eur. J.* **2019**, *25*, 11031–11035.
[32] G. Sauer, D. Nasu, D. Tietze, T. Gutmann, S. Englert, O. Avrutina, H. Kolmar, G. Buntkowsky, *Angew. Chem. Int. Ed.* **2014**, *53*, 12941–12945; *Angew. Chem.* **2014**, *126*, 13155–13159.
[33] E. Cavallari, C. Carrera, S. Aime, F. Reineri, *ChemPhysChem* **2019**, *20*, 318–325.
[34] E. Cavallari, C. Carrera, M. Sorge, G. Bonne, A. Muchir, S. Aime, F. Reineri, *Sci. Rep.* **2018**, *8*, 8366.
[35] S. Korchak, S. Mamone, S. Glöggler, *ChemistryOpen* **2018**, *7*, 672–676.
[36] R. W. Adams, J. A. Aguilar, K. D. Atkinson, M. J. Cowley, P. I. P. Elliott, S. B. Duckett, G. G. R. Green, I. G. Khazal, J. López-Serrano, D. C. Williamson, *Science* **2009**, *323*, 1708–1711.
[37] K. D. Atkinson, M. J. Cowley, S. B. Duckett, P. I. P. Elliott, G. G. R. Green, J. López-Serrano, I. G. Khazal, A. C. Whitwood, *Inorg. Chem.* **2009**, *48*, 663–670.

[38] J.-B. Hövener, N. Schwaderlapp, T. Lickert, S. B. Duckett, R. E. Mewis, L. A. R. Highton, S. M. Kenny, G. G. R. Green, D. Leibfritz, J. G. Korvink, J. Hennig, D. von Elverfeldt, *Nat. Commun.* **2013**, *4*, ncomms3946.
[39] A. Harthun, R. Giernoth, C. J. Elsevier, J. Bargon, *Chem. Commun.* **1996**, 2483–2484.
[40] R. Giernoth, P. Huebler, J. Bargon, *Angew. Chem. Int. Ed.* **1998**, *37*, 2473–2475; *Angew. Chem.* **1998**, *110*, 2649–2651.
[41] I. V. Skovpin, V. V. Zhivonitko, I. V. Koptyug, *Appl. Magn. Reson.* **2011**, *41*, 393–410.
[42] A. S. Kiryutin, G. Sauer, A. V. Yurkovskaya, H.-H. Limbach, K. L. Ivanov, G. Buntkowsky, *J. Phys. Chem. C* **2017**, *121*, 9879–9888.
[43] V. V. Zhivonitko, K. Sorochkina, K. Chernichenko, B. Kótai, T. Földes, I. Pápai, V.-V. Telkki, T. Repo, I. Koptyug, *Phys. Chem. Chem. Phys.* **2016**, *18*, 27784–27795.
[44] R. N. Hayes, R. L. Paltridge, J. H. Bowie, *J. Chem. Soc. Perkin Trans. 2* **1985**, *0*, 567–571.
[45] F. Ellermann, A. Pravdivtsev, O. Jansen, J.-B. Hövener, in *EUROISMAR2019*, Berlin, Germany, **2019**, p. 322.

Manuscript received: November 20, 2020
Revised manuscript received: December 12, 2020
Accepted manuscript online: December 15, 2020
Version of record online: February 1, 2021